

Detection of irregularities in regular patterns

Jarkko Vartiainen, Albert Sadovnikov, Joni-Kristian

Kamarainen*, Lasse Lensu, Heikki Kälviäinen

Machine Vision and Pattern Recognition Research Group, Lappeenranta University of Technology, P.O.Box 20, FIN-53851 Lappeenranta, Finland

Received: date / Revised version: date

Abstract Regular patterns, as defined in this study, are found in areas of industry and science, for example, halftone raster patterns used in the printing industry and crystal lattice structures in solid state physics. The need for quality inspection of products containing regular patterns has aroused interest in the application of machine vision for automatic inspection. Quality inspection typically corresponds to detecting abnormalities, defined as irregularities in this case. In this study, the problem of irregularity detection is described in analytical form and three different detection methods are proposed. All the methods are based on characteristics of the Fourier transform to compactly represent regular information. The Fourier transform enables the separation of regular and irregular parts of an input

Send offprint requests to:

* Corresponding author. E-mail. Joni.Kamarainen@lut.fi; Tel. +358 5 6212844; Fax. +358 5 6212899

image. The three methods presented are shown to differ in their generality and computational complexities.

1 Introduction

A 2-D regular pattern can be defined as a unit shape repeating over an image, and the repetition adheres to a set of predefined rules. Local instances of the unit shape may vary, but the variations should be small over the whole image. Repeating patterns can commonly be observed in man-made structures like brick walls, floor tiles or printed raster patterns. In nature, such repeating patterns can be observed at the molecular level in crystal structures. Defects in the structure can be detected by observing the irregularities in the repeating patterns. The detection can be very beneficial in many tasks related to quality inspection. A typical application area where regular patterns appear is halftone imaging (e.g. [1]) and a method detecting irregularity, such as finding the number of missing dots in rotogravure prints [2], could be used in quality control.

An image processing sub-field containing many similar characteristics to the study of regular patterns is texture analysis. In texture analysis, however, the most typical problem is to distinguish between different types of textures, and thus, proposed approaches favor between-texture type classification. Irregularity detection on the other hand needs within-texture type classification. Nevertheless, there are many useful texture characteristics and notations that can be used to detect irregularities, e.g. halftone dots

can be considered as texture atoms and their spacing can be represented as the spatial interrelationships between the atoms [3]. Research related to irregularity detection has been conducted in fabric defect detection (e.g. [4]), but this problem setting is too loose for missing dot detection. While the fabric defect detection is concerned about the location of possible errors, additionally it is necessary to find what is wrong in the given location. In other words, one needs to find both the locations where there are irregularities, i.e., the local unit shape appearance fails, and the kind of irregularities present, e.g., a partly or completely missing unit shape or group of them. Khalaj et al. [5] have proposed a reasonably accurate method based on frequency estimation, but their method assumes that the regular patterns are aligned in horizontal and vertical directions (allowing the use of 1-D techniques) and the estimation may thus fail for dense regular patterns in large images (high frequencies). Tsai et al. [6] also considered regular textures, but limited their approach to directed line patterns (also reduced to a 1-D technique). Several image processing methods for missing halftone dot detection have been proposed, e.g. Langinmaa [7], and Heeschen and Smith [8], but their methods are based on simple and time consuming binary level processing or template matching and have not yielded convincing results. Especially problematic are neighbouring missing dots which the methods fail to detect [8, 7].

A suitable tool for studying regularities is the Fourier transform. An image with a periodic pattern in the spatial domain contains distinct peaks in

the frequency domain. By utilizing this information, the original image can be split into two images by performing proper filtering in the frequency domain. The first image contains the ideal repeating (regular) pattern, and the second one contains only the irregularities appearing between the ideal and the original image [9]. In this study, especially regular patterns consisting of halftone dots are considered, representing regular dot patterns, and three methods from the literature are applied to detect the irregularities, two by the authors [9] and one by D. Bailey in [10]. The results can be extended to any type of regular patterns by updating the irregularity classification phase accordingly and the methods are invariant to rotation and scaling of image data. The minimum degree of irregularity to be detected can be tuned (e.g. a partly or completely missing halftone dot). The main contribution of this paper is a proper framework for defining regular patterns and a comprehensive study of the methods by comparing their strengths and weaknesses in the detection of irregularities.

2 Regular patterns

In this section we define appropriate notations for studying regularity. Throughout the section we express regular patterns as repetitions of dots, giving possibly the simplest form for the unit shape. That does not, however, restrict the generality as dot patterns are analyzed via the general lattice structure where the form of the unit cell is not restricted [11].

2.1 Pattern regularity

Regularity is a property which means that some mnemonic instances follow a set of predefined rules. In the spatial domain regularity typically means that a pattern consists of a periodic or quasi-periodic structure of smaller pattern units (atoms), and thus, it is worthwhile exploring the pattern regularity in terms of periodic functions and especially via their Fourier transforms. The following is mainly based on definitions used in solid state physics and is related to Bravais lattice formulations: A Bravais lattice is an infinite array of discrete points with an arrangement and orientation that appears exactly the same from any of the points forming the array. A two-dimensional (2-d) Bravais lattice consists of all points with position vectors \mathbf{R} of the form

$$\mathbf{R} = n_1\mathbf{a}_1 + n_2\mathbf{a}_2 \quad (1)$$

where \mathbf{a}_1 and \mathbf{a}_2 are any two vectors not on the same line, and n_1 and n_2 range through all integer values. The vectors \mathbf{a}_i are called primitive vectors and they generate (span) the lattice. It should be noted that the vectors \mathbf{a}_i are not unique. Fig. 1 shows a part of a two-dimensional Bravais lattice.

The definition of a Bravais lattice refers to points, but it can also refer to a set of vectors which represent another, preferably locally concentrated, structure. The region which includes exactly one lattice point is called the primitive unit cell and \mathbf{a}_i now define the spatial relationship of the unit cells. Unit cells can also be defined as non-primitive, but in both cases they must

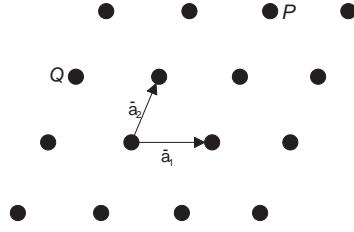


Fig. 1 A two-dimensional Bravais lattice of no particular symmetry, an oblique net. All the net points are linear combinations of two primitive vectors (e.g. $P = \mathbf{a}_1 + 2\mathbf{a}_2$, and $Q = -\mathbf{a}_1 + \mathbf{a}_2$).

fill the space without any overlapping. The primitive and non-primitive unit cells are not unique.

2.2 Fourier transform of 2-d periodic functions

Let us consider a function $f(\mathbf{r})$ (where $\mathbf{r} = (x, y)$) in which the spatial domain is a periodic extension of the unit cell. The periodicity can be formally described. Let M be a 2×2 matrix $[\tilde{\mathbf{a}}_1 \ \tilde{\mathbf{a}}_2]$ which is invertible and such that

$$f(M\mathbf{m} + \mathbf{r}) = f(\mathbf{r}) \quad (2)$$

where \mathbf{m} is any 2-dimensional integer vector. Every point \mathbf{r} in the space can be written uniquely as

$$\mathbf{r} = M(\mathbf{n} + \mathbf{u}) \quad (3)$$

where \mathbf{n} is a 2-dimensional integer vector and \mathbf{u} is a vector where each coordinate satisfies $0 \leq u_i < 1$. The unit cell $\mathcal{U}(M)$ is a region in the space corresponding to all points $M\mathbf{u}$. It can be shown that the volume (area in 2-D) of unit cell is $V = |\det M|$.

The set of all points $\mathcal{L}(M)$ of the form $M\mathbf{n}$ is called the lattice induced by M . A point in the space corresponds to a point in the unit cell translated by a lattice vector. Note that a sum of two lattice vectors is a lattice vector and the periodicity of function f implies that its value is invariant to translations by multiples of the lattice vector. A matrix $\hat{M} = [\hat{\mathbf{a}}_1 \sim \hat{\mathbf{a}}_2]$ can be obtained by inverting and transposing M , i.e.,

$$\hat{M} = M^{-T} . \quad (4)$$

For \hat{M} , a new lattice and unit cell can be associated, called the reciprocal lattice $\mathcal{L}(\hat{M})$ and the reciprocal unit cell $\mathcal{U}(\hat{M})$, respectively. If we consider the wave number space, each vector \mathbf{k} is written uniquely as

$$\mathbf{k} = \hat{M}(\boldsymbol{\kappa} + \boldsymbol{\xi}) \quad (5)$$

where $\boldsymbol{\kappa}$ is any 2-dimensional integer vector and $\boldsymbol{\xi}$ any real vector whose ordinates are $0 \leq \xi_i < 1$. The reciprocal lattice vectors span the lattice points $\hat{M}\boldsymbol{\kappa}$.

The fundamental result is that the Fourier transform of a periodic function of the unit cell specified by M is a discrete spectrum, where peaks are located at the reciprocal lattice points specified by $\hat{M}^{-1}[11]$, i.e., the wavenumber vectors are constrained to lie at the reciprocal lattice points.

The explicit transform and inverse transform formulas are

$$\hat{f}_M(\mathbf{k}) = \frac{1}{|\det M|} \int_{\mathbf{r} \in \mathcal{U}(M)} f(\mathbf{r}) e^{-j(\mathbf{k} \cdot \mathbf{r})} dV(\mathbf{r}), \quad \mathbf{k} \in \mathcal{L}(\hat{M}) \quad (6)$$

and

$$f(\mathbf{r}) = \sum_{\mathbf{k} \in \mathcal{L}(\hat{M})} \hat{f}_M(\mathbf{k}) e^{j\mathbf{k} \cdot \mathbf{r}}. \quad (7)$$

The discrete spectrum can be interpreted as a continuous spectrum consisting of Dirac impulse functions located at the reciprocal lattice points (here $D = 2$)

$$\hat{f}(\mathbf{k}) = \sum_{\boldsymbol{\kappa} \in \mathcal{Z}^D} \hat{f}_M(\hat{M}\boldsymbol{\kappa}) \delta(\mathbf{k} - \hat{M}\boldsymbol{\kappa}). \quad (8)$$

2.3 Fourier transform of 2-d quasi-periodic functions

In a more general case we can take a 2-d image which is approximately periodic (quasi-periodic). Consider a pattern image whose unit cell and lattice structures are specified by M . If this image is unbounded in all directions, and we can consider a function which is periodic (i.e., invariant of translation by the lattice vector), then the superposition of waves whose wavenumber vectors are precisely the lattice vectors in the reciprocal lattice, are specified by $\hat{M} = M^{-T}$.

However, real images have finite extent and contain imperfections (irregularities). An ideally periodic function is constrained to satisfy certain boundary conditions. We illustrate the consequences of these conditions by considering a situation where the pattern is comprised of a finite number of

translations of the unit cell. Let \mathcal{V} denote the finite region occupied by the pattern, and consider the window function $w_{\mathcal{V}}(\mathbf{r})$ defined as

$$w_{\mathcal{V}}(\mathbf{r}) = \begin{cases} 1, & \mathbf{r} \in \mathcal{V} \\ 0, & \text{otherwise} \end{cases} \quad (9)$$

If $f(\mathbf{r})$ is the ideal, the truly periodic function (with periodicity specified by M) and $f_{\mathcal{V}}(\mathbf{r})$ is the truncated function

$$f_{\mathcal{V}}(\mathbf{r}) = w_{\mathcal{V}}(\mathbf{r}) f(\mathbf{r}) = \begin{cases} f(\mathbf{r}), & \mathbf{r} \in \mathcal{V} \\ 0, & \text{otherwise} \end{cases} \quad (10)$$

then $f_{\mathcal{V}}(\mathbf{r})$ has a continuous spectrum given by

$$\hat{f}_{\mathcal{V}}(\mathbf{k}) = \sum_{\boldsymbol{\kappa} \in \mathbb{Z}^2} \hat{f}_M(\hat{M}\boldsymbol{\kappa}) \hat{w}_{\mathcal{V}}(\mathbf{k} - \hat{M}\boldsymbol{\kappa}) \quad (11)$$

where $\hat{w}_{\mathcal{V}}$ is the Fourier transform of $w_{\mathcal{V}}$.

It can be shown that $\hat{w}_{\mathcal{V}}$ contains a continuous spectrum which has infinite extent, but which fades out in proportion to $1/|\mathbf{k}|$.

The most important result is that quasi-periodic functions have quasi-discrete spectra in which the spectral energy is concentrated at the points in the reciprocal lattice.

2.4 Pattern irregularity

In terms of function periodicity, pattern irregularity can be defined as an aperiodic function $\varepsilon(x, y)$ with spatial energy $|\varepsilon| \ll |f_{\mathcal{V}}|$.

A 2-d regular pattern image can be formulated as

$$f_{\mathcal{V}}(\mathbf{r}) = w_{\mathcal{V}}(\mathbf{r}) f(\mathbf{r}) + \varepsilon(\mathbf{r}) \quad (12)$$

and the objective is to separate the regular part $w_{\mathcal{V}}(\mathbf{r}) f(\mathbf{r})$ and the irregular part $\varepsilon(\mathbf{r})$ as accurately as possible.

3 Extracting a regular pattern

As was described in the previous section, the formation of the ideal regular image is crucial for irregularity detection. The more accurate the model that can be established, the more accurate and detailed the detection that can be made.

The level of details needed for the formation is particularly high, for example, in Heliotest images [12], and thus, typical texture segmentation methods (e.g. [3]) or defect detection methods (e.g. [4]) cannot provide sufficient accuracy; the user must be able to define the minimum deviation from the single ideal unit cell which is classified as an irregularity.

A good approach to estimate the ideal regular pattern is to derive a computational analytical model and to estimate the model parameters based on the input image. This approach has been proposed, for example, in [4], but it requires a precise and very accurate analytical model, in which case the parameter estimation may become very unstable and slow. Typically, real images do not correspond to analytical models but contain distortions and noise. For this reason it is motivated to use the analytical model only as a

restricting bias in the regular pattern formation and allow incompleteness by extracting the regular pattern from the image itself. This approach has been utilized in frequency domain self-filtering to emphasize regular patterns [10] and in the methods proposed by the authors [9]. Results from the regular lattices and the reciprocal lattice are applied, but only to coarsely estimate the model parameters while details are extracted from the input image.

3.1 Spatial modeling limits of accuracy

Before considering how to extract the ideal regular pattern from the input images, it is important to understand why the parameters of the analytical model cannot be directly estimated. The analytical models would be the most obvious solutions since they are commonly used in regular dot pattern synthesis, e.g. digital halftoning [1], and in defect detection (e.g. [4]). In the context of regular dot patterns, the analytical expression in (12) can be used, but the limits of accuracy prevent estimation of the model parameters directly since practical restrictions due to the discrete image resolution cannot be bypassed. For the same reason, the limited resolution, halftone synthesis is not necessarily reversible.

Fig. 2(a) shows a simplified model of a regular dot pattern which can also be used to describe the pattern in Heliotest assessment [2,12]. The model parameters can be divided into the following classes:

1. Image geometry parameters, i.e., lattice primitive vectors \mathbf{a}_1 , \mathbf{a}_2 (see Fig~2(a)) and the overall lattice shift vector \mathbf{s} .
2. Unit cell model parameters. In the case of a Heliotest it can, for example, be a 2-d Gaussian hat (see Fig~2(b)).

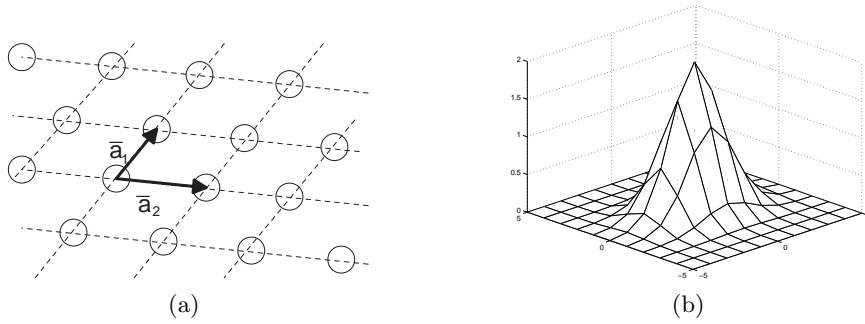


Fig.~2 Simple model of a regular dot pattern (Heliotest): (a) 2-d lattice structure ($\mathbf{a}_1, \mathbf{a}_2$ - primitive vectors); (b) Gaussian dot model (μ, Σ, A).

Accurate estimates for all parameters are necessary to generate an accurate ideal model which can be used by comparing it to or subtracting it from the observed image. However, the estimation is not trivial; it can be performed with search or generic optimization methods where the target function to be minimized is the energy difference between the observed image and the model. Unfortunately, the number of parameters to be optimized is very high and they cannot be optimized independently.

The first step in the pattern modeling is estimation of the lattice parameters ($\mathbf{a}_1, \mathbf{a}_2$) representing the periodicity (lattice matrix M). These parameters can be estimated using a number of techniques: image auto-correlation space, texture statistics (gray-level statistics), fixed window features, etc.

Problems, however, may arise, such as incorrect period estimation (convergence to harmonics nM instead of M). The only solution seems to be a good initial estimate of the period. The model estimation approach depends on the input image and further generalization seems to be of a low success.

It is also possible to estimate the parameters using statistical tools: the mean lattice matrix M_μ and lattice matrix deviation M_Σ . An important consideration is whether the mean lattice matrix could be used as the ideal lattice model. Our practical experiments, unfortunately, showed that it cannot be used; typically the observed lattice in the images is not regular enough and therefore the lattice should be modeled as a real world stochastic process. The only possible solution would be local refinement where each lattice grid point is adjusted to the corresponding unit cell in the input image. This in turn would cause additional computational expenses which would prevent efficient implementation of the method. Furthermore, it should be noted that additional model parameters introduce more uncertainty and more adjustment is then required.

It is evident that it is easy to construct a mathematical model to synthesize regular dot patterns, but this process is often irreversible in practice due to the limited acquisition resolution and exhaustive computation needed for the parameter estimation. With the help of application specific heuristics, the model parameter estimation may succeed for a specific application, but the approach can still be computationally infeasible. It is obvious that a

more general, re-usable, and sufficiently accurate approximation technique is needed.

3.2 Exploiting Fourier domain

Let us now consider real images which represent the regular dot patterns. Such images are produced by the Heliotest assessment as shown on the left-hand-side of Fig. 3. Next consider the Fourier spectra of an image, i.e., the magnitude spectra. On the right-hand-side of Fig. 3 it is possible to see the distinct frequency peaks which are located at the reciprocal lattice points in (6).

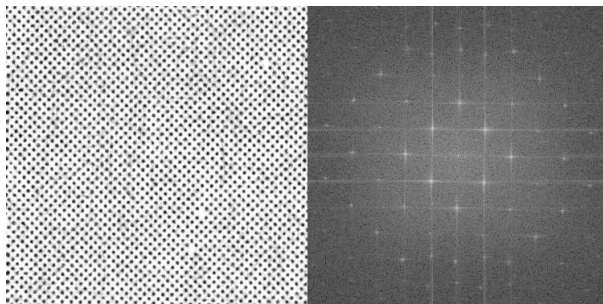


Fig. 3 Example of the regular dot pattern image (Heliotest) and its Fourier spectra magnitude.

It is clear that by filtering out the reciprocal lattice frequencies it is possible to estimate the faultless periodic component, the ideal regular pattern. The irregular parts can be afterwards obtained by subtraction. These two parts are now called the regular and irregular parts of the image (demonstrated in Fig. 4). It should be noted that effects of image borders in Fig. 4

appear since the borders are discontinuity points. Separation of the parts can be formulated as

$$\begin{aligned}
\xi(x, y) &= \mathfrak{F}^{-1}\{\Xi(u, v)\} = \\
&= \mathfrak{F}^{-1}\{\mathfrak{M}(u, v)\Xi(u, v) + (I(u, v) - \mathfrak{M}(u, v))\Xi(u, v)\} = \\
&= \underbrace{\mathfrak{F}^{-1}\{\mathfrak{M}(u, v)\Xi(u, v)\}}_{\text{regular part}} + \underbrace{\mathfrak{F}^{-1}\{(I(u, v) - \mathfrak{M}(u, v))\Xi(u, v)\}}_{\text{irregular part}}
\end{aligned} \tag{13}$$

where $\xi(x, y)$ is the spatial image, \mathfrak{F} and \mathfrak{F}^{-1} are forward and inverse discrete Fourier transforms, $\mathfrak{M}(u, v)$ is a mask filter (real valued function of the same definition domain as $\Xi(u, v)$), and $I(x, y)$ is the unit function. The decomposition in (13) is possible because of the identity of addition in the spatial and frequency domains. The mask filter can be of any type suitable for a particular application, i.e., accept/reject (binary), notch filter, etc. The only condition for the mask is that it should retain the periodic component while preserving other frequencies unchanged, i.e., it should be band-pass on frequencies near the reciprocal peak points. Proper construction of mask is the central problem in this study and will be considered in the next section.

3.3 Spatial domain vs. frequency domain

Many image processing techniques work well directly in the spatial domain. However, with repetitive patterns the choice of frequency domain is obvious. Due to the FFT algorithm, forward and inverse Fourier transforms can be performed efficiently. 2-d periodicity in the spatial domain is represented by

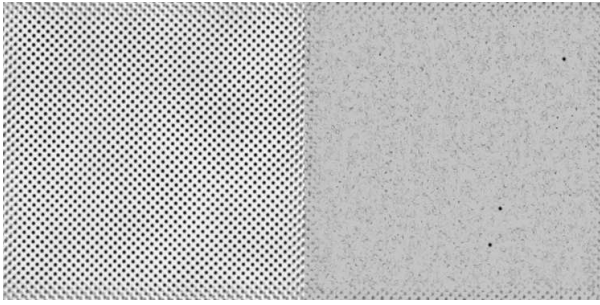


Fig. 4 Examples of regular and irregular image parts (Heliotest).

the lattice matrix M and a 2-d periodic function in the frequency domain has a discrete spectrum located at the reciprocal lattice, M^{-T} , points. For an $N \times N$ image, the FFT transform result is also $N \times N$ with discrete frequencies ranging from 0 to $(N - 1)/N$ (wave numbers $0, \dots, N - 1$). If the input image pattern contains a large number of unit cell translations, the frequency picture will be sparse containing a small number of lattice points. Consequently, rough estimation of the lattice matrix M through a reciprocal matrix M^{-T} is easier.

Inspection of small details, such as the shape of a single unit cell, is however a difficult task in the Fourier domain, and therefore, the inverse transform back to the spatial domain is needed for detailed analysis. These issues will be discussed next in the description of the algorithms we propose.

4 Irregularity detection algorithms

In this section, three different algorithms for detecting irregularities from regular patterns are introduced. The description is quite thorough, though

presented in a practical way. Before proceeding to the actual methods, it needs to be mentioned that the presented algorithms are aimed at the detection of missing dots in 2-d periodic dot patterns. In addition, the regular patterns are considered to be imaged without imaging errors, such as perspective or lens distortion.

4.1 Method based on Fourier domain regularity detection and global gray-level processing in the spatial domain

This method (referred to as method 1) is based on the fact that the periodic regular structure provides intensity peaks in the Fourier domain as demonstrated for the periodic function f and its reciprocal counterpart \hat{f} in Eqs. (2) and (8). If the mask \mathfrak{M} is automatically generated by utilizing peak locations in the frequency domain, then the regular and irregular parts can be extracted using Eq. (13). From the irregular image it is possible to find the irregularities by global processing; by thresholding the gray-level irregular image and then processing the resulting binary areas (see the right-hand-side in Fig. 3). The following stages are needed:

1. Irregular part extraction using the mask filter.
2. Global processing of the irregular image part.

These processing steps will be considered next.

4.1.1 Irregular component extraction

A general approach for the extraction of irregular component was established by the theory of reciprocal lat-

tices of periodic patterns introduced in Section 2 and by the separation principle described in Section 3.2. The extraction is described in Algorithm 1.

Algorithm 1 *Irregular image extraction*

- 1: Compute magnitude of the Fourier transform $|\Xi|$ for the input image ξ .
- 2: Find the magnitude peaks and derive the reciprocal lattice vectors $\hat{\mathbf{a}}_1, \hat{\mathbf{a}}_2$ in (4).
- 3: Create the mask \mathfrak{M} by setting (Gaussian) band-pass filters to reciprocal lattice points $\mathbf{k} = \hat{M}(\boldsymbol{\kappa})$ in (5) {Only integer steps, i.e. $\boldsymbol{\xi} = \mathbf{0}$ }.
- 4: Extract the irregular part using (13).

The first and last steps are clear enough, but the other two need more detailed description. The second step actually introduces a dual problem to the title of this study: detection of the regularity in regular patterns. The reciprocal lattice is defined by the primitive vectors $(\mathbf{a}_1, \mathbf{a}_2)$, which can be estimated with sub-pixel accuracy using the peak locations, but the estimation may be sensitive to the initial guess. The estimation ambiguity occurs due to the harmonic components, although it can be prevented using a sufficiently accurate initial guess. Another ad hoc solution would be to locate all frequency peaks, but since the frequency plane is discrete, the harmonic set estimation based on the lower frequencies is not accurate and they need to be adjusted to actual local maxima. This adjustment is performed by looking for the local maximum in certain neighbourhoods defined by the first harmonics. It should be noted that estimation to sub-pixel accuracy is not needed since the regular pattern is finally extracted from the original

image. It should be noted that in our case presence of a single regular pattern is assumed and in the case of several regular patterns the algorithm would select only the most prominent one.

Filter mask generation is based on the reciprocal lattice vectors and the band-pass filters suitable for an application. Without any prior information, the Gaussian succeeds as the general form. The width of the Gaussian can be estimated from the local peaks, but again due to the usage of the original signal in the regularity extraction, a fixed width can be safely used for efficiency. Two image components are derived from the observed image, one containing the regular image part and the other containing the irregular one. It should be noted that the algorithm tolerates arbitrary rotations and scalings.

4.1.2 Processing the irregular image The irregular image produced by Algorithm~1 must be further processed to locate which irregularities are sufficiently severe to be detected. The irregular image processing is defined in Algorithm~2.

Algorithm 2 *Detecting irregularities from irregular image*

- 1: *Threshold the irregular image ξ_I using the threshold τ .*
- 2: *Remove all foreground areas of size less than S .*
- 3: *Compute the center locations of each remaining foreground area.*
- 4: *Return the centers as irregularity coordinates.*

There are various methods which can be used to perform the binary processing tasks in steps 2 and 3, e.g. areas of size less than S can be removed using

the binary opening procedure [13]. Algorithm 2 requires two parameters to be defined: a threshold value τ and the minimum area S of irregularities. Due to the image normalization used in the previous stages, a fixed threshold value can be used. These parameter values can also be estimated using a training set.

4.2 Method based on self-filtering

Method 2 is based on frequency domain self-filtering [10]. In this approach, the frequency magnitude itself is used as the filter and the filtering is performed by multiplication in the frequency domain corresponding to the convolution in the spatial domain. If $\Xi(u, v)$ is the Fourier transform of the image $\xi(x, y)$, the filter $\mathfrak{M}_2(u, v)$ is the magnitude, i.e.,

$$\mathfrak{M}_2(u, v) = |\Xi(u, v)| \quad (14)$$

Depending on the frequency content of the original data, it might be appropriate to emphasize the high frequencies by applying [10]

$$\mathfrak{M}_3(u, v) = \sqrt{u^2 + v^2} |\Xi(u, v)| \quad (15)$$

but since this also emphasizes noise (high frequencies) (14) is used.

After the given image is filtered (multiplied) in the frequency domain, the regular and irregular image parts can be transformed to the spatial domain by the inverse Fourier transform. Now, the regular image part con-

tains the repeating pattern and the irregular image part contains nothing but the irregularities. Once the regular and irregular parts have been separated, Method 2 proceeds exactly like Method 1: the irregular image is thresholded, and the binary areas larger than the constant S are considered as irregularities.

4.3 Method based on Fourier domain regularity detection and local gray-level processing in the spatial domain

This approach (referred to as Method 3) can be divided into the following:

1. Spatial lattice estimation.
2. Local classification at the spatial lattice points in the original image.

4.3.1 Spatial lattice estimation Spatial lattice estimation corresponds to the estimation of irregularities in the regular part, and thus, Algorithms 1 and 2 can also be used to find centroids of the unit cells. The only difference is that the regular image part is used instead of the irregular one. After the centroids of regular image have been located, the original image is processed and analyzed at each unit cell location. Therefore, instead of using the centroids of the irregularities, the centroids of regularities (unit cells) are returned.

4.3.2 Local classification at spatial lattice points The centroids of each unit cell are known. At each location in the original image a decision whether the cell is regular or irregular (not missing or missing, see Fig. 5) must

be made. First, feature extraction is needed. Next, the extracted features are classified by a two-class classifier. The selection of proper features and classifier may have a significant effect on the results. Due to the simplicity of the problem in the case of missing Heliotest dots, the gray-level vector of a 7×7 image patch and a subspace classifier were used in this study [14].

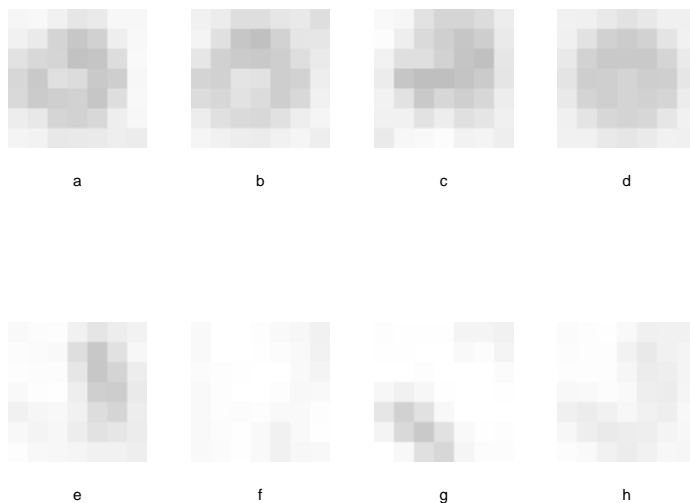


Fig. 5 Examples of dots in Heliotest images: (a)-(c) Regular dots; (d) Regular dot expectation; (e)-(g) Missing dots; (h) Missing dot expectation (note that the dot is not completely missing).

It should be noted that a separate training set is needed in this approach.

5 Experiments

In this section, the introduced methods are applied to a real machine vision problem where missing raster dots are automatically counted. All experiments were implemented in the Matlab environment running in a 2.6GHz Pentium 3 laptop with 1GB of main memory.

Paper printability is a property which describes how a certain paper type behaves in the printing process. In general, printability depends on the interactions between the paper and printing ink, and variables of the printing process itself. Good printability generally means that the paper is not sensitive to variations in the variables but always provides sufficiently good print quality. Therefore, printability describes the final result of printed images. It is clear that print quality does not have absolute terms but depends on many factors, such as the print density, resolution, and evenness of the printed image. In practice, estimation of the print quality can be generated based on several different quality assessments. [15]

In the rotogravure printing process, reproduction of light and medium tones is the greatest difficulty. In the reproduction of these tones, the two recognized defects are missing dots and waving. In the missing dot defect, the ink is not transferred to the paper. This is considered to be due to bad paper quality; the paper surface does not allow the ink to be absorbed into the paper. Missing dots are inevitable at 5% half tone, but disastrous when occurring at 20% and 30% half tones [15]. A half tone means a tone which is in between the paper color and the ink color. A specific half tone can be generated by transferring a corresponding amount of ink. In dark areas (close to ink color), missing dots are more visible. It is evident why the number of missing dots in an image area is a traditional measure of the rotogravure printability of paper. The Heliotest was developed to measure

number of missing dots and standardized for laboratory printing by the Centre Technique du Papier (<http://www.webctp.com>).

Rotogravure print samples are generated by using a special Heliotest device and the assessment itself, i.e., counting of the missing dots, is performed by visual inspection. The sample strip contains a printed dot pattern (Fig. 6(a)) which may have some of the dots missing (Fig. 6(b)). Furthermore, as can be seen in Fig. 6(a), the ink color gradually becomes lighter along the strip, which is due to the decreasing dot size in the rotogravure cylinder.

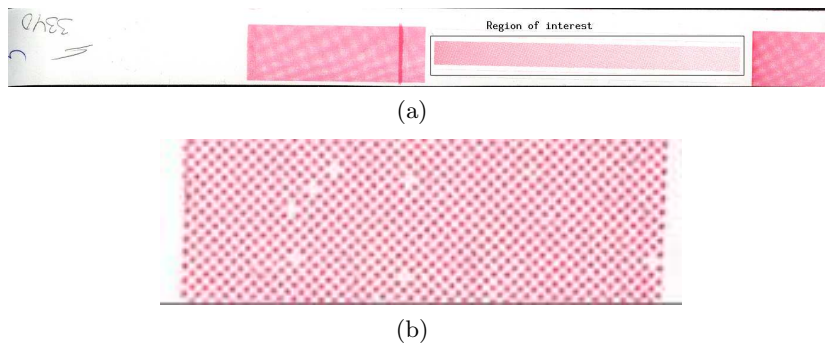


Fig. 6 Heliotest strips: (a) Example of a typical Heliotest strip, the dimensions of the region of interest are 110.0 mm by 8.5 mm; (b) Part of the strip magnified.

5.1 Measuring performance

The visual inspection introduces variance to the quality due to the subjective evaluation as to whether a single dot is missing or not. Thus an automatic assessment method would be beneficial [12]. The Heliotest dot pattern forms a visual structure which has been considered as the regular

dot pattern in this study and the methods presented above for irregularity detection can be used to detect the missing Heliotest dots.

In the experiments, a set of reproduced Heliotest strips were scanned using 1200 dpi resolution. The spacing of the raster dots was approximately 0.3~mm . The training set consisted of 75 images and the test set of 70 images. The training set was needed for Method 3 to train the two classes: dots and missing dots. Furthermore, as the parameters of the rotogravure cylinder change along the print area (ink cup size decreases producing smaller and lighter dots), the strips must be processed in separate windows.

Since the ground truth data for the missing dots was carefully collected by visually inspecting the printed strips, the comparison was done with respect to the manual selections. First, a radius from the ground truth points was defined, and if an automatically detected missing dot was found within the specified distance, the corresponding missing dot was considered to have been detected. Similarly, all automatically detected dots which were outside the specified radius were considered as false alarms. By this performance measure, the number of correct and false detections can be evaluated.

Another meaningful accuracy measure comes directly from the industry: the distance from the beginning of the strip to the 20th missing dot. Computing the locations of every missing dot would be a vague measure due to the subjective evaluation, but the distance to the 20th missing dot is shown to better correlate to the print quality. The automatic measurement should be accurate when compared to the human assessment (the ground truth)

and provide the results efficiently (human observation is approximately 5-10 seconds). It has been agreed with the industrial partners that a probability of less than 5.0% to have an error more than 10.0 mm would meet the industrial requirements.

5.2 Results

The results are reported for the proposed methods, global processing of the irregular image (Method 1), self-filtering (Method 2), and local processing of the original image (Method 3).

The number of detected missing dots and false alarms as functions of radius from the ground truth missing dots are shown in Fig. 7 for all methods. It can be seen that the local processing (Method 3) provides more accurately detected missing dots and fewer false alarms. The results are demonstrated in pixels and the mean shortest distance between two dots was 7.1 (the graphs in Fig. 7 stop at 4.0 pixels).

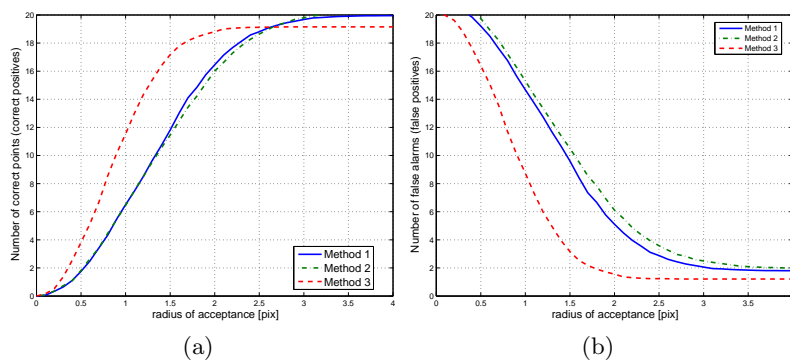


Fig. 7 Detection accuracies as functions of radius from the ground truth locations (plotted with different colors): (a) correct positives; (b) false positives.

The accuracies of all methods as compared to the ground truth 20th missing dot are shown in Fig. 8. Each method was separately used to count the missing dots from the beginning of each strip and the distance to the location of the 20th automatically detected missing dot was obtained. In this performance measure, individual false positives and false negatives contributed only to the final error. Using this industrial error measure all methods performed almost equally well. For 95% of the test samples the error remains under 8.0 mm and the required accuracy was thus met. The average execution times in the laptop PC for the methods were as follows: Method 1 - 7.76 s, Method 2 - 6.66 s and Method 3 - 49.9 s. The difference in execution times between Method 1 and Method 2 comes from the time that is needed to process the peaks in the frequency domain. It takes 0.43 s on average to detect and mask the frequency domain peaks with Method 1, whereas with Method 2 which utilizes frequency domain self-filtering the same task requires 0.15 s on average. The methods perform equally well for this industrial measurement, but it is clear from Fig. 7 that if the ground truth point were decreased from 20, then Method 3 would outperform the other two methods.

Examples of the detected missing dots (Method 2) are shown in Fig. 9. During the experiment it was found out that most of the false positives were actually correct positives, but they were missed during the manual ground truth marking. Figs. 9(c) and 9(d) show examples where the method seems to be over-sensitive detecting only partly missing dots as missing dots;

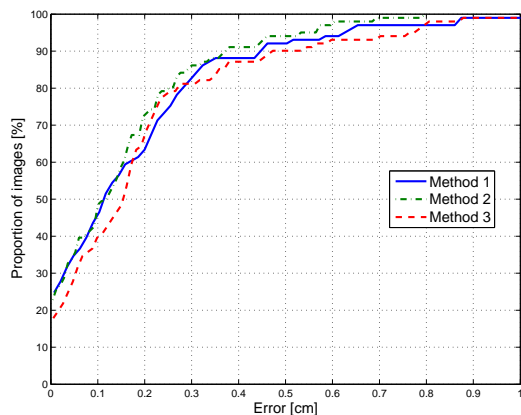


Fig. 8 Cumulative error distributions with different methods.

however in some cases those points were also considered as missing dots by an expert.

5.3 Near-regular textures

The previous experiments on Heliotest images quantitatively evaluated the accuracy of the methods, but to demonstrate generality the proposed methods were also applied to free form regular textures. Images from the CMU NRT near-regular texture database (<http://graphics.cs.cmu.edu/data/texturedb/gallery/>) were used. Method 2 was applied to several images using the common intensity threshold $\tau = 240$. Examples of the irregularity detection from near-irregular textures with artificially imposed irregularities are shown in Fig. 10.

It is clear that while the Heliotest assessment appears a straightforward application of the proposed methods and acted as the original reason for

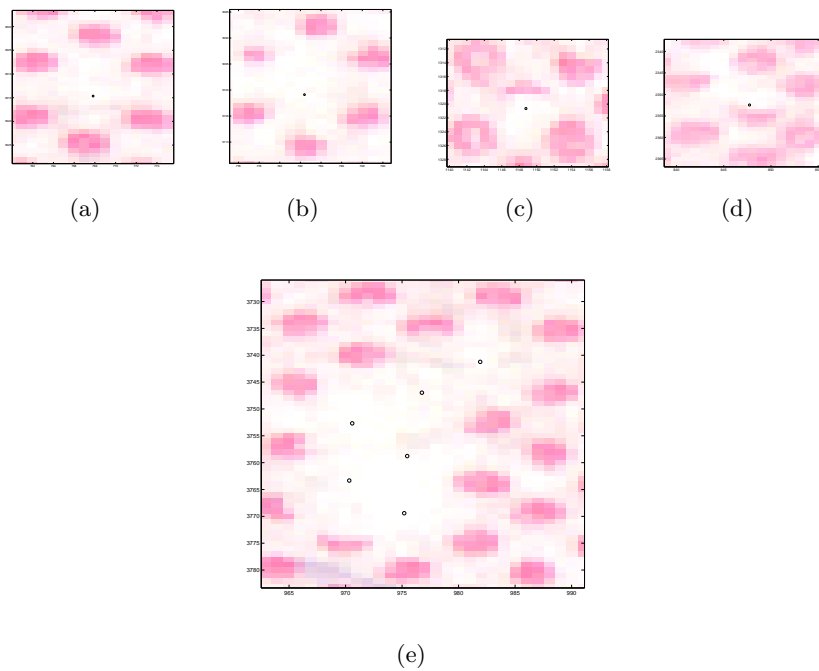


Fig. 9 Examples of detected missing dots: (a),(b) dot completely missing (correct positive); (c),(d) dot partly missing (false positive); (e) a group of missing dots (correct positives).

the research, the methods provide also a more general approach to the irregularity detection from regular and near-regular textures.

5.4 Discussion

All the presented methods are suitable for detecting irregularities from regular patterns. Methods 1 and 2 are very efficient, but they cannot in principal match the accuracy of Method 3 since it uses a classifier at each location to determine whether there is an undistorted unit cell or not. The disadvantage of Method 3 is its computing time and the requirement of a training set.

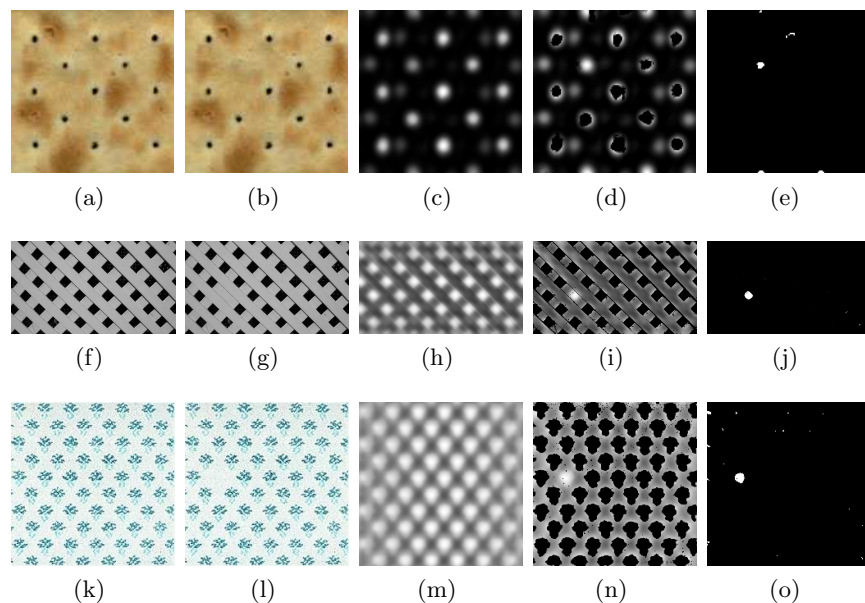


Fig. 10 Near-regular textures from CMU NRT database; (a),(f),(k) Original image; (b),(g),(l) Artificially generated irregularity; (c),(h),(m) Regular image (intensity enhanced); (d),(i),(n) Irregular image (intensity enhanced); (e),(j),(o) Thresholded irregular image.

In the practical problem of automating the Heliotest assessment all three methods performed almost equally well.

Although Methods 1 and 2 are almost identical in nature, Method 1 has advantages over Method 2. Method 1 utilizes prior knowledge of the Fourier peaks, and thus, can even detect several underlying regular patterns from the given image. For example, if the image has two repeating patterns at different frequencies, Method 1 can be used to extract either of the underlying patterns. Method 2 utilizing frequency domain self-filtering is unable to extract the two different repeating patterns, but instead locates both patterns as such. The clear advantage of Method 2 is that it needs no prior knowledge of the spatial properties of the repeating pattern.

6 Conclusions

In this study, the regular patterns were defined by using the 2-d pattern periodicity where the repeated shape, the unit cell, was considered to be dot shaped (regular dot patterns). The proposed approach can be extended to any type of unit cell, but the proposed irregularity detection methods may fail for other than compact connected areas (dots).

Based on the properties of periodic lattices and their reciprocals, three methods were introduced to accurately detect irregularities in regular dot patterns, i.e., completely or partly missing unit cell entities. All the methods assume that the input image can be divided into regular and irregular parts, and that the regular part is sufficiently strong to be detected in the reciprocal space. The first method directly utilizes the irregular part and processes it globally to detect the most visible irregularities. The second method is even more straightforward by utilizing the original image as the mask of regularity. The third method utilizes the regular part to find the centroids of all unit cells, and then locally classifies whether the cells are distorted or not. Methods 1 and 2 were shown to meet the industrial requirements for accuracy and computing time, and thus, can be used in applications where fast irregularity (defect) detection from large regular patterns is required.

Acknowledgments

Academy of Finland (project 204708) and European Union (TEKES/EAKR projects 70049/03, 70056/04 and 40483/05) are acknowledged for financial support.

References

1. H.-R. Kang, *Digital Color Halftoning*, SPIE Press, 1999.
2. P. Piette, V. Morin, J. Maume, Industrial-scale rotogravure printing tests, *Wochenblatt für Papierfabrikation* 125(16) (1997) 744–750.
3. R. M. Haralick, Statistical and structural approaches to texture, *Proc. of the IEEE* 67(5) (1979) 786–804.
4. C. H. Chan, G. Pang, Fabric defect detection by Fourier analysis, *IEEE Trans. on Industry Applications* 36(5) (2000) 1267–1276.
5. B. Khalaj, H. Aghajan, T. Kailath, Patterned wafer inspection by high resolution spectral estimation techniques, *Machine Vision and Applications* 7(3) (1994) 178–185.
6. D.-M. Tsai, C.-Y. Hsieh, Automated surface inspection for directional textures, *Image and Vision Computing* 18 (1999) 49–62.
7. A. Langinmaa, An image analysis based method to evaluate gravure paper quality, in: *Proc. 11th IAPR Int. Conf. on Computer Vision and Applications*, Vol. 1, 1992, pp. 777–780.
8. W. Heeschen, D. Smith, Robust digital image analysis method for counting missing dots in gravure printing, in: *Proc. Int. Printing & Graphic Arts Conference*, Atlanta, GA, USA, 2000, pp. 29–35.

9. A. Sadovnikov, J. Vartiainen, J.-K. Kamarainen, L. Lensu, H. Kälviäinen, Detection of irregularities in regular dot patterns, in: Proc. of the IAPR Conf. on Machine Vision Applications, Tsukuba Science City, Japan, 2005, pp. 380–383.
10. D. Bailey, Detecting regular patterns using frequency domain self-filtering, in: Proc. Int. Conf. on Image Processing, Vol. 1, Washington DC, USA, 1997, pp. 440–443.
11. N. W. Ashcroft, N. D. Mermin, Solid State Physics, Thomson Learning, Inc., 1976.
12. A. Sadovnikov, Automated Heliotest inspection using machine vision, Master's thesis, Lappeenranta University of Technology (2003).
13. R. C. Gonzalez, R. E. Woods, Digital Image Processing, Prentice-Hall, Inc., 2002.
14. E. Oja, T. Kohonen, The subspace learning algorithm as a formalism for pattern recognition and neural networks, IEEE Int. Conf. on Neural Networks 1 (1988) 277–284.
15. J.-E. Levlin, L. Söderbjelm, Pulp and Paper Testing, Papermaking Science and Technology, Fapet Oy, 1999.